

Supplementary Materials for

RGS Proteins Maintain Robustness of GPCR-GIRK Coupling by Selective Stimulation of the G Protein Subunit $G\alpha_o$

Huai-hu Chuang* and Alexander Y. Chuang

*To whom correspondence should be addressed. E-mail: huai-hu.chuang@cornell.edu

Published 21 February 2012, *Sci. Signal.* **5**, ra15 (2012)

DOI: 10.1126/scisignal.2002202

The PDF file includes:

Materials and Methods

Mathematical simulation of G protein activation for Fig. 1A

Membrane-targeted RGS constructs

Fig. S1. Deactivation kinetics of A1 or m2 for various RGS proteins.

Fig. S2. RGS4 does not stimulate β_2 -AR-stimulated $G\alpha_s$ -dependent GIRK currents.

Fig. S3. Deactivation kinetics of membrane-associated RGS box constructs.

Fig. S4. Deactivation kinetics and ACh dose-response curves of oocytes with or without the full-length RGS4N128A.

Fig. S5. Deactivation kinetics of the *lyn*-tagged R4Box and mutants.

Fig. S6. Effects of PTX treatment.

Fig. S7. RGS expression level-dependent deactivation kinetics.

Fig. S8. Increased RGS8 expression enhanced the acceleration of deactivation kinetics.

Fig. S9. GTP- γ -S induced GIRK activation in $G\alpha_{i1}$ -expressing oocyte membranes.

Fig. S10. RGS4 exhibited its GAP effect on $G\alpha_{i1}$ R178M.

Table S1. *P* values for comparison of RGS effects on current enhancement in Fig. 1D.

Table S2. *P* values for stimulatory effects on GIRK current by various membrane-targeted RGS box constructs.

References

Supplementary Materials and Methods

Mathematical simulation of G protein activation for Fig. 1A:

We mathematically modeled the activation process to qualitatively understand how a GAP protein accelerates kinetics of G-protein activation or deactivation, and affects the net production of active G-proteins. We assumed a two-state model: $C(\text{GDP} - \text{bound}) \rightleftharpoons O(\text{GTP} - \text{bound})$. We used a rate of $G\alpha$ activation (with agonist stimulation) 10-fold higher than the GTP hydrolysis rate that deactivates $G\alpha$. This is a reasonable assumption in order for neurotransmitters to produce a significant fraction of active G-proteins (~90% G protein activated, with the fraction of G-protein activated determined only by the ratios of these two kinetic constants). In the presence of RGS, we increased the GTPase rate (the reverse reaction) 20 fold, a number at the lower end of those found in the published biochemical data (1,2), to generate a current trace about one third the amplitude of the trace generated when assuming no GAP activity.

Membrane-targeted RGS constructs

Membrane-targeted RGS constructs were based on the following designs, which have been used to target various fusion proteins to the plasma membrane (3,4).

Lyn-tagged RGS Boxes (3): The nonapeptide MGCIKSKGK was attached to the N-terminal end of each RGS Box domain.

CD4 Δ -RGS Boxes (4): Human CD4 antigen with a truncation of the last 30 amino acids was fused to RGS4 Box or RGS7Box to form the CD4 Δ -RGS Boxes.

Figures

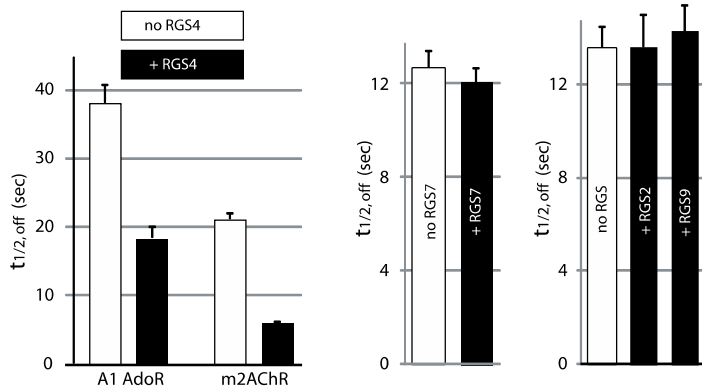


fig S1

Fig. S1. Left, deactivation kinetics of A1 or m2 reveals the GAP effect of RGS4 ($P < 0.001$). Middle and right, no significant changes were observed for deactivation kinetics of I_{KACH} in the presence or absence of RGS2, RGS7, or RGS9 ($P = 0.98, 0.59$, and 0.60 , respectively compared to oocytes not injected with RGS RNA; $n = 9-18$ oocytes).

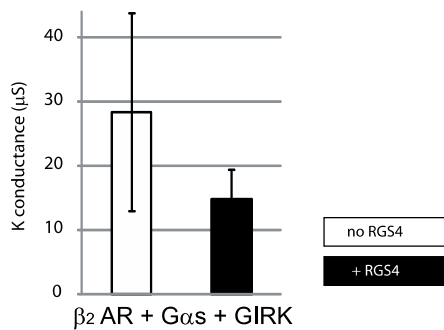


fig S2

Fig. S2. RGS4 does not stimulate β_2 -AR-stimulated $G\alpha_s$ -dependent GIRK currents ($P = 0.055$; $n = 11$ and 13 oocytes).

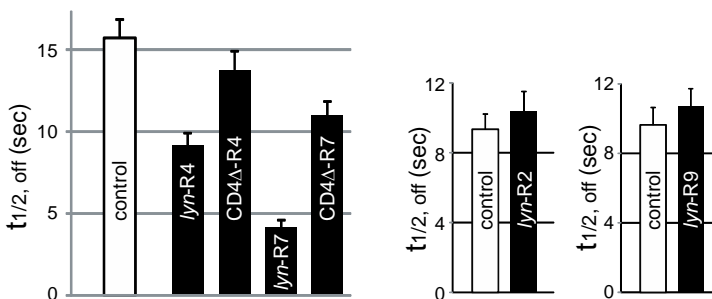


fig S3

Fig. S3. Deactivation kinetics of membrane-associated RGS box constructs with stimulatory activity (P values: *lyn*-R4Box, 0.002; CD4Δ-R4Box, 0.23; *lyn*-R7Box, < 0.001; CD4Δ-R7Box, 0.0019 compared to oocytes not injected with RGS RNA, n = 9-17 oocytes) or without stimulatory activity (P = 0.47 for *lyn*-R2Box, 0.33 for *lyn*-R9Box compared to oocytes not injected with RGS RNA, n = 12 and 9 oocytes).

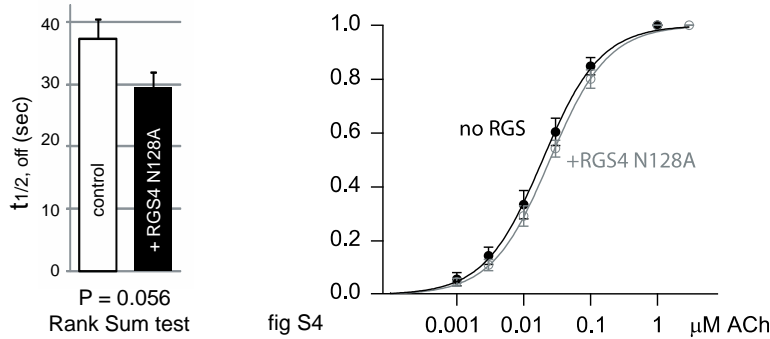


Fig. S4. Deactivation kinetics and ACh dose-response curves of oocytes with or without the full-length RGS4N128A. ΔpEC_{50} , defined as the difference between $\log\text{EC}_{50}$ (with RGS) and $\log\text{EC}_{50}$ (without RGS), is 0.066 ± 0.009 ; n = 10 oocytes.

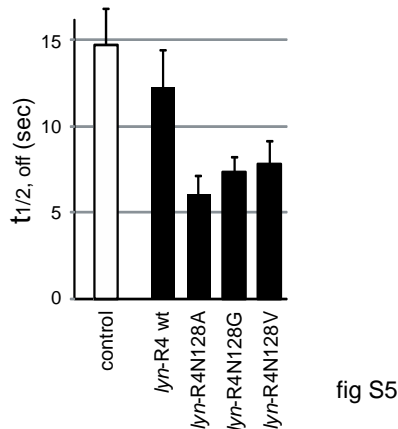


Fig. S5. Deactivation kinetics of the *lyn*-tagged R4Box and mutants (P values: *lyn*-R4Box, 0.19; *lyn*-R4BoxN128A, 0.0002; *lyn*-R4BoxN128G, 0.0011; *lyn*-R4BoxN128V, 0.009; compared to oocytes not injected with RGS RNA, n = 11 – 13).

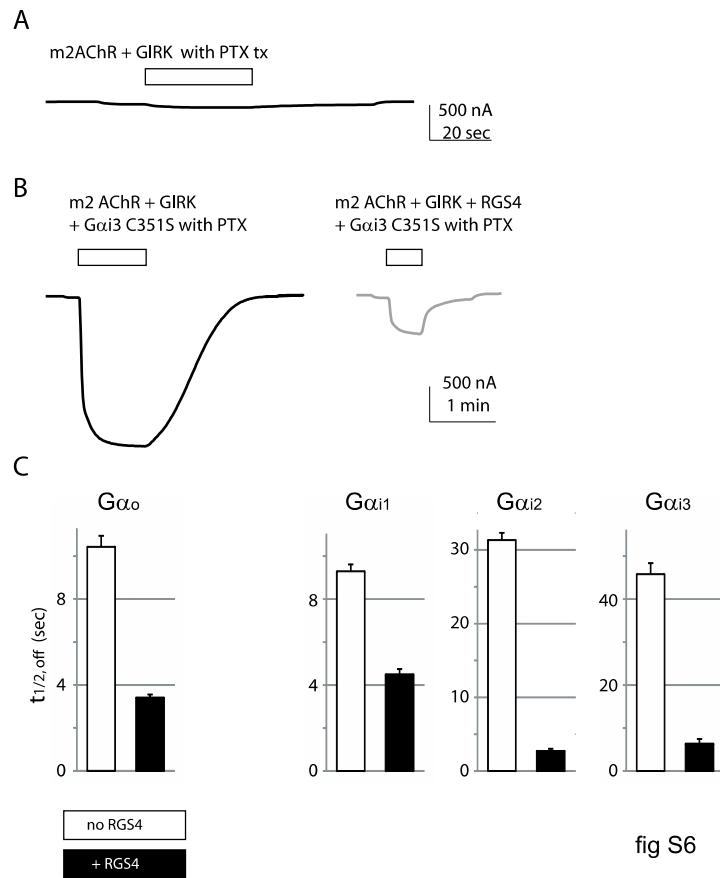


Fig. S6. Effects of PTX treatment. (A) PTX treatment abolished endogenous G-protein mediated IKACH, representative trace of $n = 5$. (B) Exogenous expression of PTX-resistant Gαi3 rescued IKACH in PTX treated oocytes, of which the deactivation kinetics was accelerated by RGS4; representative traces of $n = 9$. (C) Acceleration of deactivation kinetics of each Gα isoform by RGS4 ($P < 0.0001$ for all pairs, $n = 9 - 16$).

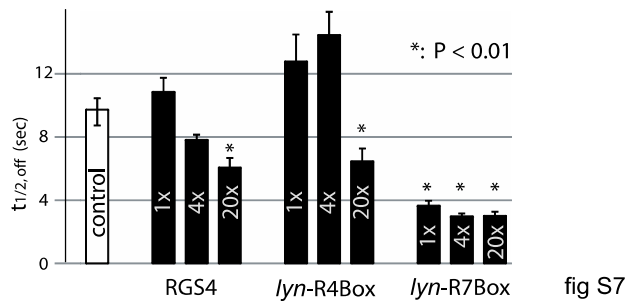


Fig. S7. RGS expression level-dependent deactivation kinetics. Acceleration of deactivation kinetics by RGS depends on the amount of mRNA injected ($n = 10 - 17$; asterisks indicate $P < 0.01$.) RGS4 4x had a P value of 0.015. RGS4 1x, lyn-R4Box 1x or 4x was not significantly different from the control.

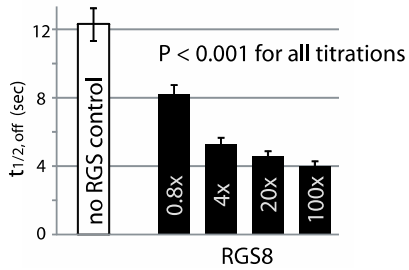


fig S8

Fig. S8. Increased injection of RGS8 mRNA (between 0.8 and 100x, where 1 x = 18.4 pg cRNA per cell) enhanced the acceleration of deactivation kinetics (from 0.8 to 100x); n = 12 – 17.

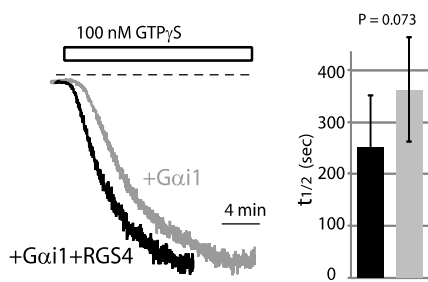


Fig S9

Fig. S9. GTP- γ -S induced GIRK activation in $G\alpha_{i1}$ -expressing oocytes membranes (compared to those from oocytes expressing $G\alpha_o$ alone shown in Fig. 8) even when RGS4 was co-expressed. The acceleration by RGS4 was below statistical significance ($P = 0.073$, n = 5).

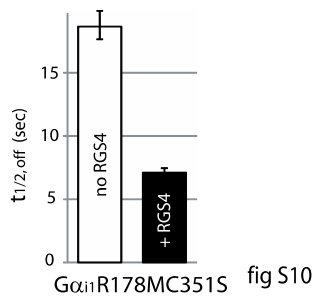


fig S10

Fig. S10. RGS4 exhibited its GAP effect on $G\alpha_{i1}$ R178M ($P < 0.0001$), n = 8 and 11.

Tables

Pair for comparison	Fold stimulation	P value
RGS(-) vs RGS2(+)	1.8	0.018
RGS(-) vs RGS4(+)	6.5	2.6×10^{-5}
RGS(-) vs RGS7(+)	1.2	0.095
RGS(-) vs RGS8(+)	5.0	2.8×10^{-6}
RGS(-) vs RGS9(+)	0.9	0.17
RGS2(+) vs RGS4(+)	n/a	1.6×10^{-5}
RGS2(+) vs RGS8(+)	n/a	2.8×10^{-5}

Table S1: *P* values (unpaired Student's *t* tests) for comparison of RGS effects on current enhancement in Fig. 1D (n = 9-12 oocytes for each isoform).

RGS constructs	Fold stimulation (Compared to no RGS injection)	P value
RGS4 BOX (20x cRNA)	1.8	0.0068
<i>lyn</i> -R2Box	1.5	0.14
<i>lyn</i> -R4Box	3.1	$<1 \times 10^{-4}$
<i>lyn</i> -R7Box	3.0	2×10^{-4}
<i>lyn</i> -R8Box	3.3	2×10^{-4}
<i>lyn</i> -R9Box	1.1	0.067
CD4Δ-R4Box	4.9	$<1 \times 10^{-4}$
CD4Δ-R7Box	3.6	$<1 \times 10^{-4}$
1x membrane-targeted R4Box constructs vs 20x R4Box	P value (for the increase in stimulation efficiency)	
<i>lyn</i> -R4Box	3.7×10^{-2}	
CD4Δ -R4Box	3.2×10^{-2}	

Table S2: *P* values for stimulatory effects on GIRK current by various membrane-targeted RGS box constructs (unpaired Student's *t* tests, n = 7-18). The increased stimulation of GIRK current amplitudes by the membrane-targeted R4Box (1x) constructs compared to the RGS4Box

(20x), was apparent as greater current stimulation of ACh-activated GIRK current by membrane-targeted RGS by a smaller amount of injected RNA.

Supplementary References

1. Srinivasa SP, Watson N, Overton MC, Blumer KJ. Mechanism of RGS4, a GTPase-activating protein for G protein alpha subunits. *J Biol Chem* **273**, 1529-1533 (1998).
2. Posner BA, Mukhopadhyay S, Tesmer JJ, Gilman AG, Ross EM. Modulation of the affinity and selectivity of RGS protein interaction with G alpha subunits by a conserved asparagine/serine residue. *Biochemistry* **38**, 7773-7779 (1999).
3. Zacharias DA, Violin JD, Newton AC, Tsien RY. Partitioning of lipid-modified monomeric GFPs into membrane microdomains of live cells. *Science* **296**, 913-916 (2002).
4. Gu C, Jan YN, Jan LY. A conserved domain in axonal targeting of Kv1 (Shaker) voltage-gated potassium channels. *Science* **301**, 646-649 (2003).